MODELED MASS AND TEMPERATURE EFFECTS OF ENTRAINED SNOW ON THE LUBRICATED FLOW REGIME AND IMPLICATIONS FOR PREDICTING AVALANCHE RUNOUT DISTANCE

Katreen Wikstrom Jones[1, 2]*, Michael G. Loso[2, 3], and Perry Bartelt[4]

[1] *Alaska Division of Geological & Geophysical Surveys, Fairbanks, AK, USA*
[2] *Department of Environmental Science, Alaska Pacific University, Anchorage, AK, USA*
[3] *Wrangell-St. Elias National Park and Preserve, Copper Center, AK, USA*
[4] *WSL Institute for Snow and Avalanche Research SLF, Davos, Switzerland*

ABSTRACT: Understanding how the snow cover in an avalanche path may impact avalanche flow behavior is essential to predict an accurate avalanche runout. In avalanche paths with strong elevational snow temperature gradients it is common for multiple flow regimes to develop within one avalanche. We demonstrate the role of snow entrainment for the development of fluidized and lubricated flow regimes and their effects on avalanche runout. We simulated avalanches in the avalanche runout model RAMMS on a 2 m resolution digital elevation model of a long, continuous, 30° (average) avalanche slope in maritime south-central Alaska, to examine how mass and temperature of released and entrained snow affect the lubricated wet flow regime and therefore avalanche runout distances. We found that meltwater production was the predominant contributing factor to long runout distances due to reduced basal friction as the avalanche makes the transition from the fluidized to the lubricated flow regime. The temperature of entrained snow was most important when the entrained mass was large relative to the released mass, and small increases in snow temperature (e.g. from -3°C to -1°C) could drastically enhance avalanche runout. Based on our results, we suggest that avalanche forecasters working in subarctic climates closely monitor warming snow cover temperatures, especially during weather events that could rapidly warm the snow, e.g., rain or strong solar radiation during the spring months.

KEYWORDS: Snow Entrainment, Avalanche Runout, Flow Regime, Fluidization, Lubrication

1. INTRODUCTION

Predicting avalanche runout distances is difficult in an operational environment because of the challenge to accurately estimate the effects of snow entrainment. Although it is long recognized that snow entrainment is the cause of avalanche growth (Sovilla et al., 2007) and observations indicate that entrainment plays a critical role in governing avalanche runout (Hamre, 2014, pers. comm.), it remains unclear exactly how entrainment causes flow regime transitions; that is, how entrainment amplifies flow states associated with fluidized (mixed flowing/powder avalanches) or wet avalanche flow regimes. Recent research efforts have demonstrated the significant role played by temperature of entrained snow (Steinkogler et al., 2014; Vera Valero et al., 2015). Depending on the temperature of the avalanche core, it has been shown that the entrained snow temperature could either have a warming or cooling effect. In addition to temperature, the mass of the entrained snow, relative to the mass of the avalanche core, dictates the magnitude of warming or cooling, and affects avalanche momentum and friction. The temperature and mass of entrained snow therefore influence the development of dry and wet flow regimes (Vera Valero et al., 2015).

In this model-based study, we examined how changes in mass and temperature of released and entrained snow influenced avalanche flow regimes and runout distances. We simulated 332 avalanches in the 2-D dynamical avalanche runout model RAMMS, using terrain that represented a steep avalanche path with a small starting zone, typical for the fjord-like topography in south-central Alaska. We used a 2 m resolution terrain surface, based on Bird Hill's avalanche path Whiskey located along the Seward Highway between Anchorage and Girdwood in south-central Alaska (60°57'1.42"N, 149°16'5.28"W). The methodology consisted of a model calibration phase (3.1), followed by numerical experiments (3.2). We discuss the warming effects of a warming snow cover (4.1), energy dissipation from frictional shear and granular fluctuations (4.2), avalanche mass (4.3), and the role of terrain in directing flow during different flow regimes (4.4).

* *Corresponding author address:*
Katreen Wikstrom Jones
Div. of Geol. & Geophys. Surveys
3354 College Rd
Fairbanks, AK 99709, United States;
tel: +1 907-451-5006;
email: katreen.wikstromjones@alaska.gov

2. MODELING WARM SNOW ENTRAINMENT IN RAMMS

Modelling avalanche (Φ) interaction with an erodible substrate (Σ) is a long standing problem in snow engineering, see Figure 1.

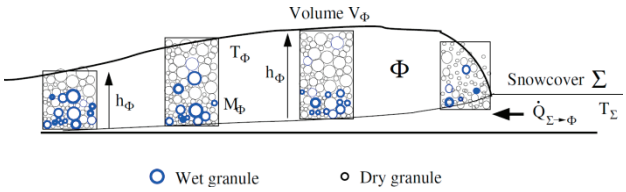

Figure 1: Wet snow avalanche. Thermal heat energy is entrained by the avalanche when it erodes the snow cover. Meltwater is concentrated on the granule surfaces.

The avalanche core temperature can vary between the avalanche front to tail, but in the model we consider a mean avalanche core temperature T_Φ that is constant over the avalanche flow height h_Φ. This assumption implies that we can calculate the overall change in internal heat energy, but not the exact temperature within the avalanche depth or for individual snow granules. We postulate constitutive relations describing how the avalanche core behaves as the mean temperature and mean water content of the avalanche increase.

For entrainment we define a constitutive relationship describing how much snow is entrained by the avalanche. We postulate that the snow entrainment rate at the avalanche front $\dot{M}_{\Sigma\to\phi}$ (kg m^{-2} s^{-1}) is controlled by the density ratio of the snow layer density ρ_Σ, the slope-parallel velocity of the avalanche u_ϕ and the erodibility parameter κ (unitless), the latter to be defined by the model user (Christen et al., 2010):

(Eq. 1)

$$\dot{M}_{\Sigma\to\phi} = \kappa \rho_\Sigma u_\phi$$

The denser the snow and the faster the avalanche is moving, the more mass is entrained (Eq. 1). We explicitly avoid the definition of a strength parameter; we assume that the avalanche can entrain all snow that it encounters in the path. The amount of heat influx from the entrained snow to the avalanche core is defined by the snow cover temperature T_Σ.

In RAMMS we model the internal heat energy E_Φ of the avalanche according to the balance equation (see Vera Valero, et al, 2015, or Bartelt et al, 2018, in these proceedings),

(Eq. 2)

$$\frac{\partial(E_\Phi h_\Phi)}{\partial t} + \frac{\partial(E_\Phi h_\Phi u_\Phi)}{\partial x} + \frac{\partial(E_\Phi h_\Phi v_\Phi)}{\partial y} = \dot{Q}_\Phi + \dot{Q}_{\Sigma\to\Phi} + c_\Sigma \dot{M}_{\Sigma\to\Phi} \dot{T}_\Sigma$$

The temperature of the avalanche core T_Φ is related to the internal heat energy by the specific heat c_Φ,

(Eq. 3)

$$E_\Phi = \rho_\Phi c_\Phi T_\Phi$$

In Eq. 2 we can identify the three most important effects on internal heat energy:

(1) Warming of the snow by dissipation of frictional energy $\dot{Q}_\Phi$. This is a function of the shear work $S_\Phi \cdot u_\Phi$. (S_Φ: shear resistance, u_Φ: avalanche velocity).

(2) Influx of heat energy by snow entrainment, $c_\Sigma \dot{M}_{\Sigma\to\Phi} \dot{T}_\Sigma$ where $\dot{M}_{\Sigma\to\Phi}$ is the mass of entrained snow and c_Σ is the specific heat of the entrained snow.

(3) The energy dissipation of the entrainment process $\dot{Q}_{\Sigma\to\Phi}$. This is discussed in detail in Bartelt et al., 2018 of these proceedings.

The most important constitutive influence of temperature is the production and decay of random energy $\dot{P}_\Phi$. Energy which is not directly dissipated to heat E_Φ is non-directional random kinetic energy R_Φ. The amount of heating $\dot{Q}_\Phi$ at any given time or position in the avalanche core is explained by this relationship (Buser and Bartelt, 2009),

(Eq. 4)

$$\dot{P}_\Phi = (\alpha)[S_\Phi \cdot u_\Phi] - \beta R_\Phi h_\Phi$$
$$\dot{Q}_\Phi = (1-\alpha)[S_\Phi \cdot u_\Phi] + \beta R_\Phi h_\Phi$$

The production of random energy $\dot{P}_\Phi$ is responsible for slope-perpendicular forces in the avalanche core which change the avalanche flow density. When the avalanche is cold, the production rate *α* of random energy $\dot{P}_\Phi$ from fluctuating and colliding snow granules is high which makes the core behave like a fluid, referred to as the fluidized regime (Bartelt et al., 2016). When the avalanche core gets warmer and granules mold together, the decay rate *β* increases, which terminates the fluidized regime (Vera Valero et al., 2015). Due to inelastic granular interactions, i.e. granule rubbing, collisions, abrasions, etc., all *R* that is produced in the core will dissipate to heat (Buser and Bartelt, 2009). This energy dissipation occur on the granule surface resulting in higher temperatures on the surface than in the granule interior. Therefore, meltwater will begin to be produced *before* the mean avalanche temperature reaches $T_\Phi = 0°C$ (Figure 1). We make the assumption that meltwater remains bonded to the granules, which physically implies that meltwater is concentrated in regions where it is produced, for example at shear surfaces. The accumulation of meltwater, trapped in the mass of heated surfaces, causes a rapid decrease in shear strength and therefore flow friction. Consequently, avalanche flow friction is a function of shearing S_Φ,

random kinetic energy R_Φ, temperature T_Φ and water content. Once the avalanche core exceeds 0°C and starts to produce meltwater, RAMMS is set to automatically assign the static (surface) friction μ a significantly reduced value (μ_{wet}= 0.12) to represent the gliding (low friction) of the lubricated regime (Vera Valero et al., 2015).

3. METHODS

3. 1 Model calibration

In the model calibration phase, we assigned values to all RAMMS friction and flow regime parameters that were not going to be tested in the numerical experiments, including static friction μ, turbulent friction ξ, constant cohesion N, erodibility coefficient κ, production rate of random kinetic energy α, and activation energy R_0. First, we tested the sensitivity of runout distance to these input parameters by using the one-at-a-time testing technique of varying the value of one parameter per avalanche simulation and keeping all other parameters constant (Hamby, 1984).

Second, we reconstructed three historical avalanche events that occurred in Whiskey, seeking to maximize the fit between simulated and observed avalanche runout, and to obtain fitted values for the friction and flow regime parameters (see 3.2 for fitted values). Available data for all three events included avalanche type (e.g., soft slab or wet slab), release depth, runout distance, and debris volume on the highway, whereas other information varied in availability and quality. Very little information was available about the snow conditions in the release area and the path. To estimate values for these input parameters, we collected historical weather data from local weather stations as well as from the monthly snow reports provided by National Resources Conservation Services. We investigated air temperatures, wind speeds, and accumulated snow depths between each snow cycle, and compared these to the reported release depths in the avalanche events in Whiskey in order to extrapolate snow depths. Based on this analysis, we estimated values for the input release and snow entrainment parameters. In each simulation trial we first plugged in our estimated values for the release and snow entrainment parameters. For the tunable friction and flow regime parameters we started with a set of values (the typically-used values for the type of avalanche, for example, higher initial α value for colder releases than for warmer releases, and lower μ for warm releases than for colder releases), and ran simulations one at a time to monitor how the output variables were affected by each value change. We ran simulations until an avalanche was generated that agreed with, first of all, our known runout distance, and then roughly with the measured deposition width and height on the highway and/or railroad. This evaluation process was restricted by the lack of information for each event and the low accuracy of the existing data. In any case, we stopped running simulations when the whole range of possible values for each tunable parameter had been fitted, and the "winning" simulation had the most matching output to the real event.

3. 2 Experimental design

For our experimental avalanche simulations (n=332) we defined snow cover parameters to represent typical snow cover conditions for subarctic maritime climates where a strong snow temperature gradient from sea level to ridge tops is prevalent (see Wikstrom Jones et a., 2016, for parameter values used). We simulated avalanches by changing a release or entrained snow characteristic one at a time, with other parameters kept constant. We defined two snow entrainment zones: a high zone above 500 m asl and a low zone below 500 m asl. We gave each zone a snow depth with the physical assumption that the snow depth was either the same or decreased with drop in elevation. We defined snow temperatures with the assumption that snow temperature was either the same or became warmer with drop in elevation. We did not account for any atmospheric temperature inversions long-lived enough to invert snow temperatures. The temperatures of released snow and entrained snow were paired with a density, resulting in increased mass with increase in temperature. If the zone had a snow cover we set the static friction μ to 0.55 and turbulent friction ξ to 1200 ms^{-2}, and for bare ground 0.65 and 1400 ms^{-2}. Cohesion N was set to 50 Pa for -8°C releases, 75 Pa for -5°C, and 100 Pa for -1°C and 0°C. We used erodibility coefficient k 0.3, granule density 450 kg/m^3, and wet snow RKE regime with 2.0 kJm^{-3} activation energy R_0 for all simulations, with decreasing kinetic energy production rate α from 0.06 for -8°C and -5°C releases, to 0.05 for -3°C and 0°C releases.

4. RESULTS AND DISCUSSION

4. 1 Warming effects of warming snow cover

The results of the numerical experiments showed that meltwater production was the most important predictor of long runout distances. In general, early and rapid meltwater production was initialized by warm release-snow temperatures. Warm snow temperatures in the high entrainment zone, associated with the same or even warmer snow temperature in the low zone, was the second most important variable for early onset of meltwater production.

Entrainment of cold (≤ -3°C) snow in the lower elevations, made the very small (< 10,000 m^3) releases remain cold throughout the flow and stop early. Entrainment of warm (≥ -1°C) snow in the path made the same releases warm up quickly and become lubricated, resulting in long runout distances (Figure 2). Also, with warm snow temperatures in the path of ≥ -1°C, a slight increase in release snow temperature (for example from -5°C to -3°C) could dramatically increase the runout distance (Figure 2). For a practical application, this means that once the snow in the low zone warms up to around -1°C, it becomes very critical to monitor the snow temperatures in the higher elevations to make accurate assessments of runout distance.

4. 2 *Warming effects of energy dissipation from frictional shear and granule fluctuations*

In avalanche paths of significant drop height, the avalanche accelerates quickly, leading to high production rates of random kinetic energy; this energy will dissipate to heat. In steep terrain, heat dissipation from frictional shearing may sufficiently warm up the avalanche core for the avalanche to transition from fluidization into lubrication, independent of entrained snow temperatures in the lower elevations (Wikstrom Jones et al., 2016). This explains why the magnitude of lubrication not only depends on influx of warm snow from entrainment but also on dissipated heat from frictional shearing, and is therefore strongly affected by terrain. The amount and duration of random kinetic energy *R* production in the high zone appeared critical in determining the warming of avalanche core temperature for medium-warm releases (-3°C) that entrained consistently cold (-3°C) snow in the path. Due to their smaller size, small avalanches produced less heat kinetically during fluidization in the high zone, and would therefore remain cooler as they entrained cold snow in the low zone. For larger release volumes, the larger amounts of dissipated heat from random kinetic energy, warmed up their avalanche cores to 0°C and initiated meltwater production.

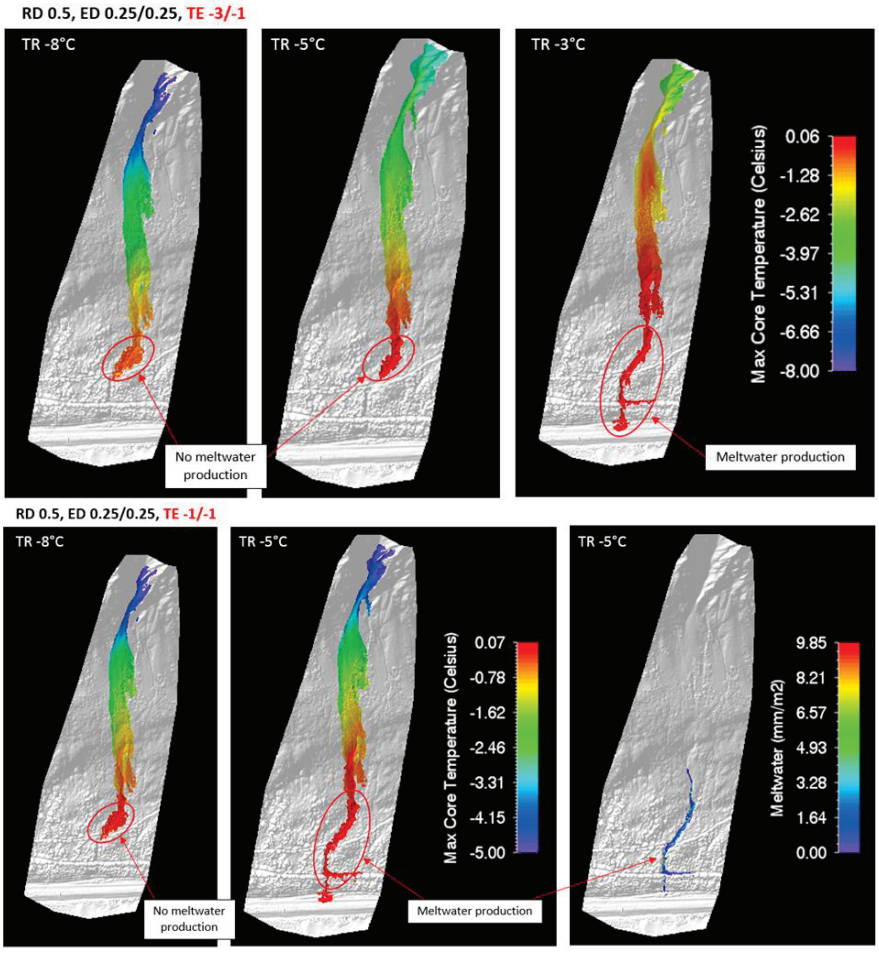

Figure 2: Effects of released (TR) and entrained (TE) snow temperature on maximum avalanche core temperature and runout distance. The depths (ED) and temperatures (TE) of entrained snow in the high zone and low zone (slash mark "/") are consistent in a given row. Color bar of Max Core Temperature (°C) is consistent for all panels in a given row.

4. 3 Warming effects of avalanche mass

The size of the simulated avalanche release mattered for how efficiently entrained snow could alter the current flow regime, i.e., warm up or cool down the avalanche. The smallest releases were very responsive to snow temperatures in the path; warm entrained snow warmed up the avalanche quickly and initiated meltwater production, whereas cold entrained snow kept it cool and prevented meltwater production. Larger releases had delayed flow regime transitions resulting from entrained snow. However, due to large amounts of dissipated heat from fluidization in the high zone, larger (> 15,000 m^3) -3°C releases were able to reach 0°C in their core despite entrainment of cold snow in the low zone.

4. 4 Effects of terrain features on avalanche flow

Our results showed that the terrain in the low zone had the ability to both facilitate and disrupt avalanche flow, depending on whether the avalanche was lubricated, fluidized, or mixed (partly fluidized, partly lubricated). These parts of the slope-perpendicular avalanche column interact very differently with the underlying terrain; wet snow tends to be directed by terrain, whereas drier, turbulent snow tends to chaotically collide and override terrain obstacles in a straighter flow path. A gully feature in the lower elevation of Whiskey constricted the avalanche mass, further enhancing lubrication and resulting in long runout distances. Mixed larger avalanches split into two separate debris tongues as they reached a sharp curve in the gully in the lower elevations and starved with short runout distances.

5. CONCLUSIONS

We adopted a numerical modeling approach to examine the effects of mass and temperature of released and entrained snow on avalanche flow behavior in steep terrain. The results showed that meltwater production was the dominant contributing factor to long runout distances, due to reduced basal friction as the avalanche makes the transition from the fluidized to the lubricated flow regime. The factors that enhanced warming of the avalanche core and production of meltwater were (1) Warmer released snow cover; (2) Warmer entrained snow in the avalanche path, especially when the mass of entrained snow is large relative to the mass of released snow; (3) Energy dissipation to heat from frictional shearing and granule fluctuations in the high zone; and (4) Frictional heat production caused by path drop height and terrain roughness. The results demonstrated that small avalanche releases were more responsive to the snow conditions in the path than larger release volumes, as they warmed up faster or remained cooler, depending on the entrained snow temperatures, and were only able to enter the lubricated regime with entrainment of warm snow. Based on our results, we suggest to avalanche forecasters working in subarctic maritime snow climates to closely monitor snow cover temperatures, especially around weather events that could rapidly warm up the snow (e.g., rain or strong solar radiation during the spring months), to prepare for longer-than-expected runout distances.

ACKNOWLEDGEMENTS

We would like to thank Eeva Latosuo, David Hamre, Marc Christen, and Cesar Vera Valero. Thank you to Alaska Railroad Corporation, SLF, Cora Shea Memorial Fund, American Alpine Club, American Avalanche Association, and Avalanche Canada Foundation for financial support. We would also like to thank Matt Murphy, Timothy Glassett, Jim Kennedy, Jason Geck, Mike Dunn, Henry Münter, Wendy Wagner, Alexander Jones, and Lauren Rocco. Lastly, thank you Beaded Stream, Alpine Air, and Fugro for your support.

REFERENCES

Bartelt, P., O. Buser, O., Vera Valero and Y. Bühler, 2016. Configurational energy and the formation of mixed flowing powder snow ice avalanches, Ann. Glaciol. 57(71): 179-187

Buser, O., Bartelt, P., 2009. Production and decay of random kinetic energy in granular snow avalanches. J. Glaciol. 55, 189.

Christen, M., Kowalski, J., Bartelt, P., 2010. RAMMS: Numerical simulation of dense snow avalanches in three-dimensional terrain. Cold Reg. Sci. Technol, 63, 1-2, 1 – 14

Hamby, D. M., 1994. A review of techniques for parameter sensitivity analysis of environmental models. Env. Monit. and Assess., 32, 135-154

Sovilla, B., Margreth, S., Bartelt, P., 2007. On snow entrainment in avalanche dynamics calculations. Cold Reg. Sci. Technol. 47, 69-79

Steinkogler, W., Sovilla, B., Lehning, M., 2014 Influence of snow cover properties on avalanche dynamics. Cold Reg. Sci. Technol. 97, 121-131

Vera Valero, C., Wikstroem Jones, K., Bühler, Y., Bartelt, P., 2015. Release temperature, snow-cover entrainment and the thermal flow regime of snow avalanches. J. Glaciol. 61, 225

Wikstrom Jones, K., Loso, M., Bartelt, P., 2016. Modeled mass and temperature effects of released and entrained snow on the lubricated regime of avalanches at Bird Hill, southcentral Alaska. Proceedings of the International Snow Science Workshop. Breckenridge, CO